

Short Communication

Sub-3 nm Pd-graphene Nanosheets with Outstanding Electrocatalytic Oxidation of Formic Acid

Junzhi He¹, Junhong Zhao¹, Zhen Run¹, Shasha Zheng¹ and Huan Pang^{1,2}

¹ College of Chemistry and Chemical Engineering, Anyang Normal University, Anyang, 455002, Henan, P. R. China.

² State Key Laboratory of Coordination Chemistry, Nanjing University, Nanjing, 210093, Jiangsu, P. R. China.

*E-mail: huanpangchem@hotmail.com

Received: 12 August 2014 / Accepted: 15 September 2014 / Published: 29 September 2014

Pd-graphene nanosheets are synthesized by a mild condition. Structures and morphologies of samples are characterized by transmission electron microscopy (TEM) images, and field-emission scanning electron microscope (FE-SEM). The concentration of N₂H₄ affects the size of Pd nanocrystals. More importantly, the size of nanocatalyst greatly affects its electrochemical activity towards electrocatalytic oxidation of formic acid. We find that the sub-3 nm Pd-graphene nanosheets exhibit much higher formic acid oxidation activity.

Keywords: Electrocatalytic oxidation of formic acid; Pd-graphene nanosheets

1. INTRODUCTION

Considerable researches have recently focused on the synthesis of uniformly sized and shape-controlled nanoparticles due to their potential applications in catalysis, electrochemistry, ion exchange, molecular adsorption, electronics, especially for magnetic properties, are very sensitive to shape variation because of the dominant role of anisotropy in magnetism. [1-17] Graphene is a single-atom-thick sheet of hexagonally arrayed sp²-bonded carbon atoms exhibiting extremely high specific surface area, and has emerged with interesting physical and chemical properties. As a new star of carbon nanomaterials, many groups are trying to investigate the potential applications in this system. [18-24] Dispersion of metal nanocrystals on graphene sheets potentially provides a new way to develop catalytic, magnetic, and optoelectronic materials.

Direct formic acid fuel cell (DFAFC), as a promising application of next generation green energy resource, has attracted many attentions in past years. [25-27] Pd based nanocatalysts have been

reported to show high activity for formic acid oxidation. [28, 29] The recent emergence of graphene nanoelectronics has opened a new avenue for utilizing 2-dimensional carbon material as a support in PEM fuel cells. [30, 31] Hope to employ such 2-D sheets as conductive mats to both anchor electrocatalysts and modulate the electrochemical reactions in a controlled fashion. As the size of nanocatalyst greatly affects its electrochemical activity, [32, 33] it is important to develop a mild synthesis route for Pd-graphene before studying its mechanism for formic acid oxidation.

Generally, size-controlled noble-metal based nanocatalysts are synthesized by wet-chemistry steps. In this work, we have succeeded in using chemically modified graphene sheets to support palladium nanocrystals of sub-3 nm diameter. More importantly, we found that the sub-3 nm Pd-graphene nanosheets exhibited much higher formic acid oxidation activity.

2. EXPERIMENTAL SECTION

Characterizations: Transmission electron microscopy (TEM) images were captured on the JEM- 2100 instrument microscopy at an acceleration voltage of 200 kV. The morphologies of the samples were taken by a Hitachi S-4800 field-emission scanning electron microscope (FE-SEM) at an acceleration voltage of 10.0 KV. All of electrochemical tests were performed at Solarton 1287 (English).

Preparation of individual graphene oxide: Graphene oxide (GO) was prepared from purified natural graphite according to a modified Hummers' method. [34] Graphite powder (1 g), NaNO_3 (0.75 g) and KMnO_4 (3 g) in concentrated H_2SO_4 (75 mL) were vigorously stirred at room temperature for 7 days. On the completion of the reaction, 5% H_2SO_4 (200 mL) aqueous solution was added, and the temperature was kept at 98 °C for 2 h. Then the temperature was reduced to 60 °C, H_2O_2 (30%, 6 mL) was added and the reaction was further stirred for 2 h. The above mixture was centrifuged to collect the bottom product and sequentially washed with 5% H_2SO_4 /0.5% H_2O_2 (15 times), 5% HCl solution (5 times), and then washed repeatedly with distilled water until the pH of the supernatant was neutral. Finally the material was dried to obtain a loose brown powder.

Synthesis of sub-3 nm Pd-graphene nanosheets (Denoted Pd-G-1): 0.05 g GO, 5 g L^{-1} SBDS 5 mL, glycol 5 mL, PdCl_2 0.01 g were mixed together, and then was ultrasonic dispersed for 15 minutes. 85 % N_2H_4 1 mL was added into the above system and stirred for 24 hours at room temperature. The reaction product was filtered and washed extensively with water and ethanol.

Synthesis of 8 nm Pd-graphene nanosheets (Denoted Pd-G-2): 0.05 g GO, 5 g L^{-1} SBDS 5 mL, glycol 5 mL, PdCl_2 0.01 g were mixed together, and then the mixture was ultrasonic dispersed for 15 minutes. 85 % N_2H_4 5 mL was added into the above system and stirred for 24 hours at room temperature. The reaction product was filtered and washed extensively with water and ethanol.

Preparation of the working electrode: The working electrode was prepared as follows: 5 mg of the catalyst was mixed with 1 mL of ethanol and 50 μL of 5 wt% Nafion solution (Du Pont). The mixture was sonicated for 30 min to obtain inky slurry. Approximately 25 μL of the slurry was applied to the surface of the glassy carbon electrode to form a thin layer of ca. 0.1256 cm^2 in geometrical area.

A saturated calomel electrode (SCE) and a Pt foil were used as the reference electrode and the counter electrode, respectively. All of tests were performed at Solartron 1287 (English).

3. RESULTS AND DISCUSSION

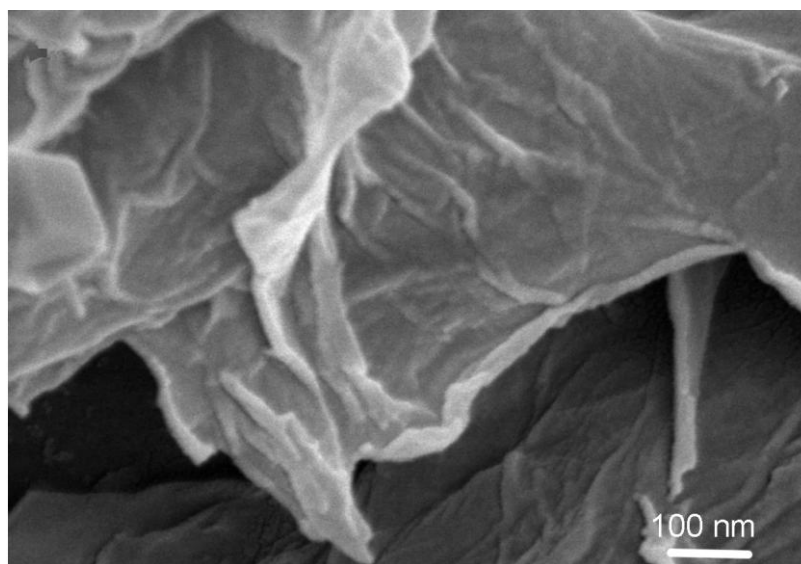


Figure 1. An SEM image of as-prepared samples.

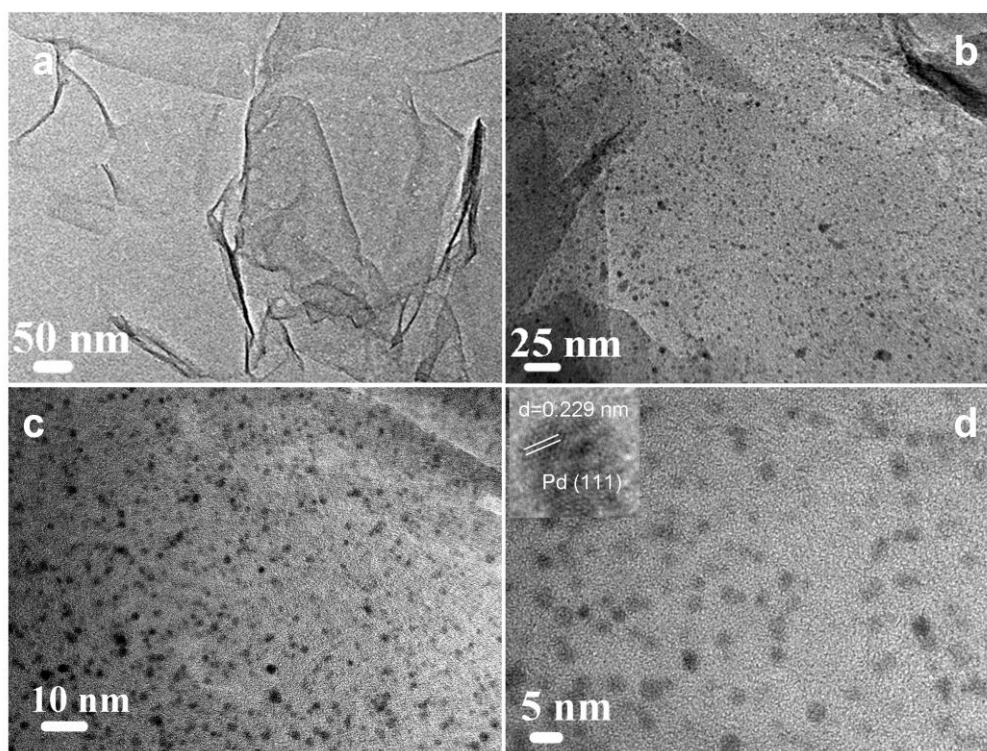


Figure 2. TEM images of as-prepared samples, a) GO nanosheets; b-d) Pd-G-1.

Graphene oxide (GO) was prepared from purified natural graphite according to a modified Hummers method. [34] The morphology of the graphene oxide was observed by SEM and TEM analysis. From Figure 1, an SEM image of the graphene oxide shows GO nanosheets are soft and can easily be imbedded small nanocrystals.

Figure 2a shows a general view of GO nanosheets, it clearly illustrates the flake-like shapes of graphite oxide and has high specific surface to be modified. We can easily see the morphology of the partly Pd-graphene nanosheets (Pd-G-1) in Figure 2b. From Figure 2c, a large number of Pd nanocrystals are dispersed on graphene sheets, and the size of these Pd nanocrystals is uniform about sub-3 nm. To further reveal the fine structure of the Pd nanocrystal, high-resolution TEM (shown in inset of Figure 2d) analysis has also been carried out, and the clear lattice image demonstrates the well-defined lattice fringes of Pd (111).

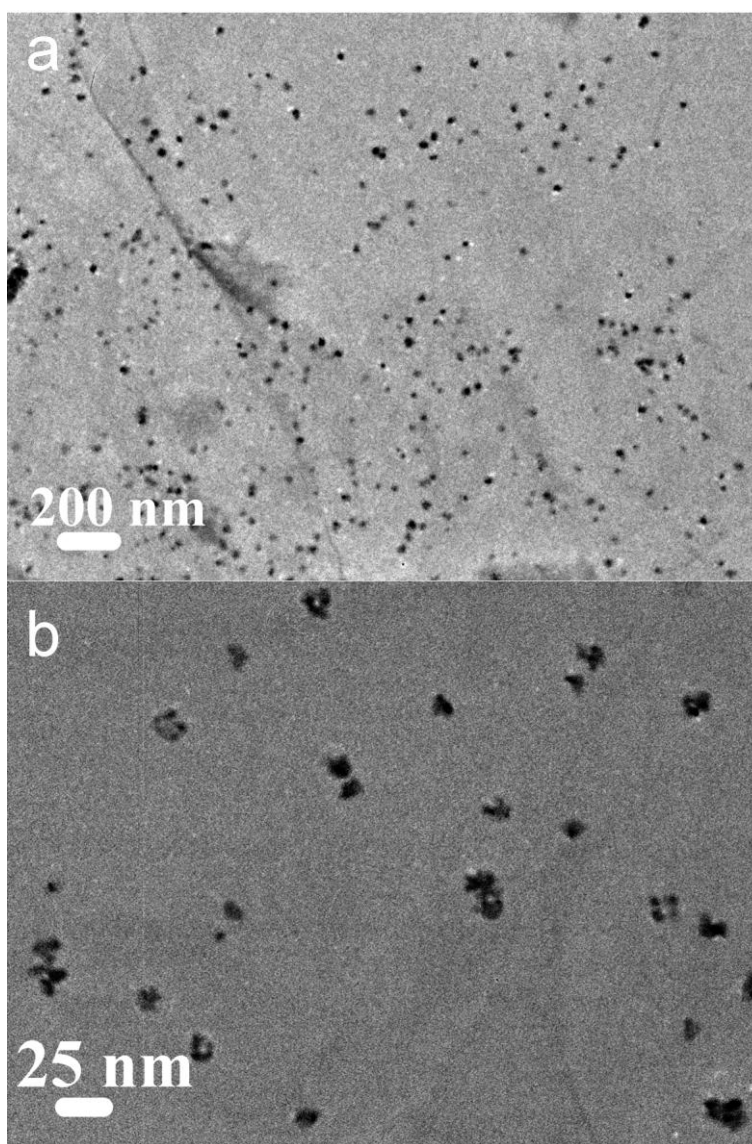


Figure 3. TEM images of as-prepared Pd-G-2.

Figure 3 shows the TEM images of Pd-G-2. A large number of Pd nanocrystals are dispersed on graphene sheets, which is the same as the Pd-G-1 in Figure 2b. However, after further magnification in Figure 3b, we can see that the size of single Pd nanoparticles is about 8 nm. The different sizes of two as-prepared samples may be result from the increasing amount of reducer- N_2H_4 for Pd-G-2.

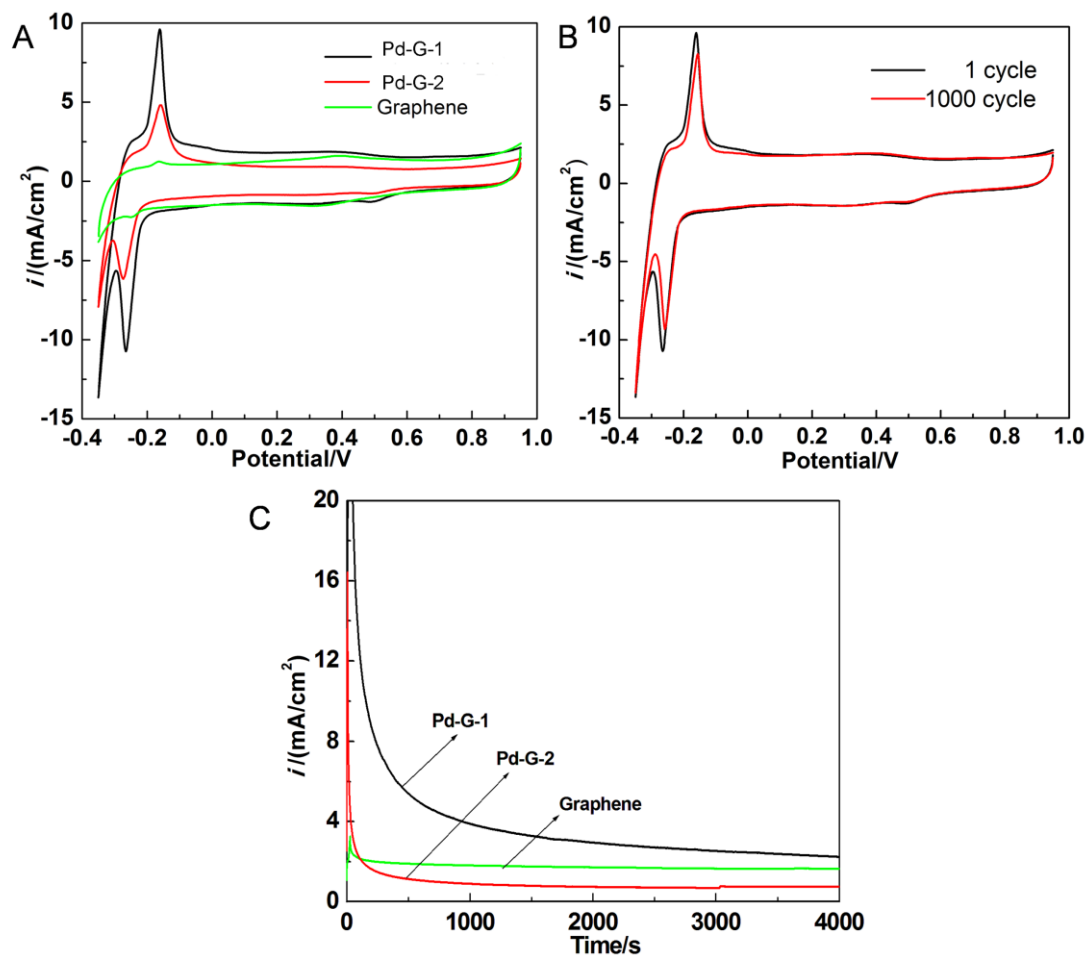


Figure 4. A) The cyclic voltammograms in 0.5 M H_2SO_4 solution on different electrodes; B) The 1st and 1000th cycle cyclic voltammograms of Pd-G-1 electrode; C) Current density-time curves of the catalysts measured by chronoamperometry in 0.5 M H_2SO_4 electrolyte.

Figure 4a shows the cyclic voltammograms in 0.5 M H_2SO_4 solution on different electrodes. It is found that the hydrogen adsorption and desorption peaks on sub-3 nm Pd-graphene nanosheets (Pd-G-1) electrode are larger than that on the 8 nm Pd-graphene nanosheets electrode (Pd-G-2) at ca. -1.61 V and -1.58 V vs. SCE, respectively. The coulombic charges of the hydrogen desorption peaks for the Pd-G-1 and Pd-G-2 catalysts are 9.66×10^{-3} and 4.80×10^{-3} A cm^{-2} respectively. And it is observed from Figure 4a that Pd-G-1 and Pd-G-2 electrodes deliver reduction peaks at ca. -1.61 V and -1.58 V, respectively, attributing to the reduction of the oxide formed on the Pd-graphene during the forward scan ($2H_2O + 4e^- = O_2 + 4H^+$). [35, 36] The stability of different electrodes is shown Figure 4b, it is

evident that Pd-G-1 electrode has good stable electrochemical behavior in 0.5 M H₂SO₄ solution. The peak current of 1000 cycle is 90 % of that of the first cycle. From Figure 4c, it also proves that the Pd-G-1 electrode has the best stable electrochemical behavior in our experiment. We can see the current density of the Pd-G-1 after 4000 s is higher than that of Pd-G-2 at the corresponding time.

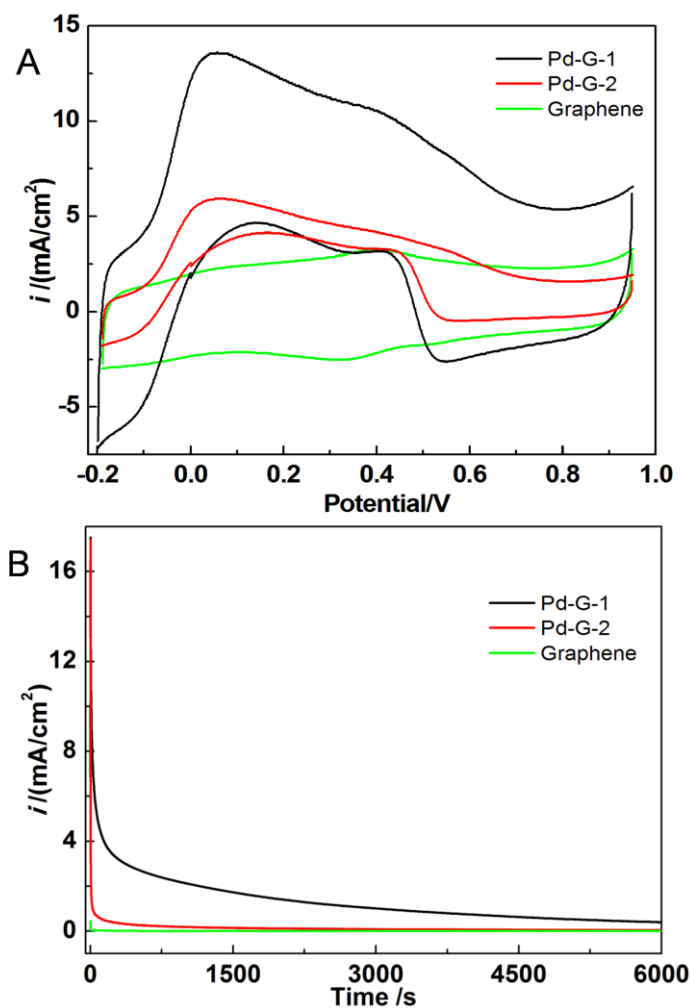


Figure 5. A) Cyclic voltammograms of as-prepared catalysts tested in the mixed solution containing 0.5 M HCOOH + 0.5 M H₂SO₄ at a scan rate of 25 mV s⁻¹; B) Current density–time curves of the catalysts measured by chronoamperometry in 0.5 M HCOOH + 0.5 M H₂SO₄ electrolyte at 0.10 V vs. SCE.

Figure 5a is a comparison of FA oxidation on the catalysts with different electrodes. The strong oxidation peaks belong to the oxidation of FA and the corresponding intermediates. From the curve, the main oxidation peak potential in the positive-scan direction for the Pd-G-1 catalyst is located at ca. 0.046 V. And the corresponding peak current density is ca. 13.5 mA cm⁻², displays the highest catalytic activity for FA. FA oxidation current density is shown to change in the order: Pd-G-1 > Pd-G-2. The corresponding oxidation peak current densities on these catalysts are 13.5, 6.0 mA cm⁻², respectively

The stability of FA oxidation on Pd-G-1 and Pd-G-2 electrodes are investigated in 0.5 M H₂SO₄ containing 0.5 M HCOOH at a constant potential of 0.1 V. The rapid current decrease shows

the poisoning of the electrocatalysts. Figure 5b shows that, the current density of the Pd-G-1 after 6000 s is higher than that of Pd-G-2 at the corresponding time. Nevertheless, at the same time, the oxidation current is larger on Pd-G-1 than that on Pd-G-2. This indicates that the certain content of sub-3 nm Pd nanocrystals-graphene which enhances the stability and poisoning tolerance of Pd. [37-40]

4. CONCLUSION

In summary, we have successfully synthesized sub-3 nm Pd-graphene by a facile route. Our method is mild and one pot, which might be used into synthesizing others metal-graphene composites. The electrochemical measurement of sub-3 nm Pd-graphene shows that the sub-3 nm Pd-graphene is an effective and stable electrocatalyst. It is a good example to prove that physical and chemical properties of nano/microstructured materials are related with their structures, and the precise control of morphology of nanomaterials will serve for controlling the performance. Dispersion of metal nanocrystals on graphene sheets potentially provides a new way to develop novel catalytic materials. Exploring the electrochemical characteristics of novel nano/micromaterials might direct a new generation of catalytic materials.

ACKNOWLEDGEMENTS

This work is supported by the Program for New Century Excellent Talents of the University in China (grant no. NCET-13-0645) and National Natural Science Foundation of China (NSFC-21201010, U1304504), Program for Innovative Research Team (in Science and Technology) in University of Henan Province (14IRTSTHN004), the Science & Technology Foundation of Henan Province (122102210253, 13A150019, 14B150001), and the China Postdoctoral Science Foundation (2012M521115). We are very grateful to *Liang Chen* from Anyang Normal University in the language modification.

References

1. Y. N. Xia and P. D. Yang, *Adv. Mater.* 15, (2003) 351.
2. Q. Song and Z. J. Zhang, *J. Am. Chem. Soc.* 126, (2004) 6164.
3. J. Cheon, N. J. Kang, S. M. Lee, J. H. Lee, J. H. Yoon and S. J. Oh, *J. Am. Chem. Soc.* 126, (2004) 1950.
4. H. Zeng, P. M. Rice and S. X. Wang, *J. Am. Chem. Soc.* 126, (2004) 11458.
5. W. G. Lu, J. Y. Fang and K. L. Stokes, *J. Am. Chem. Soc.* 126, (2004) 11798.
6. A. R. Armstrong and P. G. Bruce, *Nature* 381, (1996) 499.
7. Y. F. Shen, R. P. Zerger, R. N. Deguzman, S. I. Suib, L. Mccurdy, D. I. Potter and C. L. Oyoung, *Science*, 260 (1993) 511.
8. M. C. Bernard, H. L. Goff and B. V. Thi, *J. Electrochem. Soc.*, 140 (1993) 3065.
9. R. Jothiramalingam, B. Viswanathan and T. K. Varadarajan, *Catal. Commun.*, 6 (2005) 41.
10. J. T. Zhang, Y. Tang, K. Lee and M. Ouyang, *Nature*, 466 (2010) 91.
11. X. H. Zhang, Y. N. Li and C. B. Cao, *J. Mater. Chem.*, 22 (2012) 13918.
12. G. X. Zhu and Z. Xu, *J. Am. Chem. Soc.*, 133 (2011) 148.
13. J. F. Liu, L. L. Wang, X. M. Sun and X. Q. Zhu, *Angew. Chem. Int. Ed.*, 49 (2010) 3492.

14. X. F. Xia, Q. L. Hao, W. Lei, W. J. Wang, D. P. Sun and X. Wang, *J. Mater. Chem.*, 22 (2012) 16844.
15. M. Han, Q. Liu, J. H. He, Y. Song, Z. Xu and J. M. Zhu, *Adv. Mater.*, 19 (2007) 1096.
16. H. Pang, Y. Y. Liu, Y. H. Ma, G. C. Li, Y. N. Ai, J. Chen, J. S. Zhang and H. H. Zheng, *Nanoscale*, 5 (2013) 503.
17. H. B. Wu, H. Pang and X. W. Lou, *Energy Environ. Sci.*, 6 (2013) 3619.
18. K. Geim and K. S. Novoselov, *Nat. Mater.*, 6 (2007) 183
19. S. P. Pang, H. N. Tsao, X. L. Feng and K. Mullen, *Adv. Mater.*, 21 (2009) 1
20. H. Zhang, X. J. Lv, Y. M. Li, Y. Wang and J. H. Li, *ACS Nano*, 4 (2010) 380
21. G. Eda, H. E. Unalan, N. Rupesinghe, G. A. J. Amaratunga and M. Chhowalla, *Appl. Phys. Lett.*, 93 (2008) 233502.
22. J. T. Robinson, F. K. Perkins, E. S. Snow, Z. Q. Wei and P. E. Sheehan, *Nano Lett.*, 10 (2008) 3137
23. X. Wang, L. Zhi and K. Mullen, *Nano Lett.*, 8 (2008) 323; L. Wang, C. G. Tian, H. Wang, Y. G. Ma, B. L. Wang and H. G. Fu, *J. Phys. Chem. C*, 114 (2010) 8727.
24. H. A. Becerril, J. Mao, Z. F. Liu, R. M. Stoltenberg, Z. N. Bao and Y. S. Chen, *ACS Nano*, 2 (2008) 463.
25. M. Baldauf and D. M. Kolb, *J. Phys. Chem.*, 100 (1996) 11375.
26. X. G. Li and I. M. Hsing, *Electrochim. Acta*, 51 (2006) 3477.
27. X. W. Yu and P. G. Pickup, *J. Power Sources*, 182 (2008) 124.
28. P. K. Babu, H. S. Kim, J. H. Chung, E. Oldfield and A. Wieckowski, *J. Phys. Chem. B*, 108 (2004) 20228.
29. Z. L. Liu, L. Hong, M. P. Tham, T. H. Lim and H. X. Jiang, *J. Power Sources*, 161 (2006) 831.
30. B. Wang, J. Yang, L. Wang, R. Wang, C. Tian, B. J. Jiang, M. Tian and H. G. Fu, *Phys. Chem. Chem. Phys.*, 15 (2013) 19353 .
31. J. Yang, C. Tian, L. Wang and H. G. Fu, *J. Mater. Chem.*, 21 (2011) 3384.
32. K. Kinoshita, *J. Electrochem. Soc.*, 137 (1990) 845.
33. T. Frelink, W. Visscher and J. A. R. Vanveen, *J. Electroanal. Chem.*, 382 (1995) 65.
34. N. I. Kovtyukhova, P. J. Ollivier, B. R. Martin, T. E. Mallouk, S. A. Chizhik, E. V. Buzaneva and A. D. Gorchinskiy, *Chem. Mater.*, 11 (1999) 771.
35. G. H. El-Nowihy, A. M. Mohammad, M. M.H. Khalil, M. S. El-Deab, *Int. J. Electrochem. Sci.*, 9 (2014) 5177.
36. K. Jiang, H.-X. Zhang, S. Zou and W.-B. Cai, *Phys. Chem. Chem. Phys.*, (2014) DOI: 10.1039/C4CP03151B
37. Q. Yuan, D.-B. Huang, H.-H. Wang, Z.-Y. Zhou and Q. X. Wang, *CrystEngComm*, 16 (2014) 2560.
38. Y. Y. She, Z. G. Lu, W. G. Fan, S. Jewell and M. K. H. Leung, *J. Mater. Chem. A*, 2 (2014) 3894.
39. S. J. Li, Y. F. Shi, L. Liu, L. X. Song, H. Pang and J. M. Du, *Electrochimica Acta*, 85 (2012) 628.
40. S. J. Li, J. Z. He, M. J. Zhang, R. X. Zhang, X. L. Lv, S. H. Li and H. Pang, *Electrochimica Acta*, 102 (2013) 58.